Solution Reactivity Studies for Identification of Promising New ALD and Pulsed-CVD Reaction Chemistries

B. Vidjayacoumar[a], V. Ramalingam[a], D. J. H. Emslie[a], J. M. Blackwell[b], and S. B. Clendenning[b]

[a] Department of Chemistry, McMaster University, Hamilton, Ontario, L8S 4M1, Canada
[b] Intel Corporation, RA3-252, 2511 NW 229th Ave., Hillsboro, OR 97124, USA

Solution screening reactions are described for a range of copper(II) and nickel(II) precursors in combination with the co-reagents $AlMe_3$, $ZnEt_2$, BEt_3, Si_2Me_6, Sn_2Me_6 and $B_2(Pin)_2$ (Pin = pinacolate). These screening reactions were used to identify particularly promising precursor/co-reagent combinations for copper or nickel metal deposition, and subsequent ALD/pulsed-CVD studies are described for selected cases. NMR spectroscopic studies focused on elucidating the reaction pathways responsible for copper metal deposition from solution are also described. This manuscript reviews and expands upon previously reported work (B. Vidjayacoumar, D. J. H. Emslie, J. M. Blackwell and S. B. Clendenning *et al.*, *Chem. Mater.*, 2010, **22**, 4844-4853 and 4854-4866).

Introduction

Atomic Layer Deposition (ALD) offers a route to highly conformal thin films of uniform and controlled thickness. Thin metal films have a variety of potential applications, for example in integrated circuits, magnetic information storage, fuel cells and catalysis. However, metal ALD is less readily achieved than metal oxide or nitride ALD, especially using thermal methods as opposed to plasma enhanced methods.(1, 2)

The most common co-reagents to achieve metal ALD are H_2 and O_2. However, the latter is only suitable for the noble metals, and many ALD chemistries require high temperatures (>200 °C) which limits the number of compatible metal precursors (since CVD must be avoided), prevents ALD on less thermally robust substrates, and can cause agglomeration leading to discontinuous films. The scope of potential substrates is then further reduced by the non-selectively reducing or oxidizing nature of H_2 and O_2, respectively. As a consequence, there is a clear need for new ALD/pulsed-CVD reaction chemistries that employ alternative co-reagents and operate at lower temperatures.(3)

Herein we discuss the use of solution deposition studies as a means to identify particularly promising metal precursor / co-reagent combinations for the development of new metal ALD or pulsed-CVD reactivity. This approach is rapid and straightforward, unlike more time and resource intensive ALD/pulsed-CVD studies. Solution studies also allow for comparatively more facile analysis of the reaction pathways responsible for metal deposition, thereby providing a starting point for consideration of the reaction pathways involved during ALD or pulsed-CVD. While the extent to which solution reaction pathways correlate with those in metal ALD has rarely been determined, solution thermolysis reactions employed in the study of CVD have in some cases provided strong evidence for mechanistic parallels between solution- and surface-based reactivity.(4-7)

Experimental

General procedures have been reported elsewhere and complexes **1**-**8** and **19**-**27** were prepared as previously described.(3, 8) Emerald green anhydrous **9** (a trimer in the solid state) (9) was obtained by repeated sublimation of pale blue-green $Ni(acac)_2(H_2O)_x$. Complexes **10**,(10) **11**,(11) and **13** (12) were prepared as previously described. Complex **12** was prepared similarly to literature reports.(13, 14) Complex **14** was prepared in 70 % yield by a modification of the literature procedure:(15) reaction of the lithiated ligand with $NiCl_2$(dme) in toluene for 4h at 55 °C, followed by recrystallization from diethylether. Complex **15** was prepared as reported,(16) but using $NiCl_2$(dme) in place of $NiBr_2(THF)_{1.67}$. Complex **16** (17) was prepared following the general procedure reported by Akitsu and Einaga.(18) Following the literature, **17** was prepared from $Ni(acac)_2$ in 30% yield as a red solid,(19) and **18** was prepared from $NiCp_2$ in 70% yield as a purple liquid.(20) [$NiCl_2$(dme)] was prepared as described in the literature.(21) Si_2Me_6 was purchased from Aldrich Chemicals, distilled from molecular sieves, and stored under argon. Sn_2Me_6 (packaged in an ampoule) and B_2Pin_2 were purchased from Aldrich Chemicals and used as received. Nickel-coated silicon wafers were prepared as follows: native oxide was removed from a Si wafer using dilute HF followed by deionized water rinse and dry. Substrates were then coated with 15 nm of Ni sputtered in a standard tool using 100W DC power and a 2" Ni target with 180 sccm Ar to produce 6.5 mTorr of pressure. For ALD/pulsed-CVD studies, delivery temperatures of 120 °C and 160 °C were used for precursors **6b** and **7**.

Results and Discussion

Solution screening reactions are described for a range of copper(II) and nickel(II) precursors in combination with the co-reagents $AlMe_3$, $ZnEt_2$, BEt_3, Si_2Me_6, Sn_2Me_6 and $B_2(Pin)_2$. These screening reactions were used to identify particularly promising precursor/co-reagent combinations for copper or nickel metal deposition, and subsequent ALD/pulsed-CVD studies are described for selected cases. NMR spectroscopic studies focused on elucidating the reaction pathways responsible for metal deposition from solution are also described. A portion of the copper chemistry has previously been reported;(3, 8) the current manuscript reviews and expands upon this work.

Metal precursors

Both copper(II) and nickel(II) precursors were investigated. All copper precursors were homoleptic CuL_2 coordination complexes (Figure 1). Nickel precursors included NiL_2 coordination complexes and cyclopentadienyl complexes as shown in Figure 2. Complexes **1**-**18** were selected to represent a variety of different ligand types, differing in donor-set, the extent of electron delocalization, and steric/electronic properties.

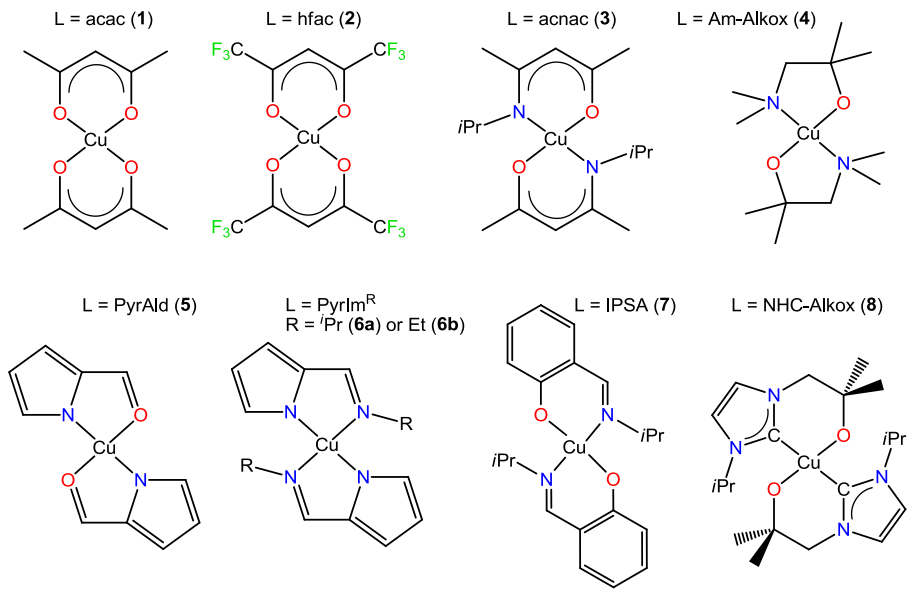

Figure 1. Homoleptic copper(II) complexes **1**-**8**.

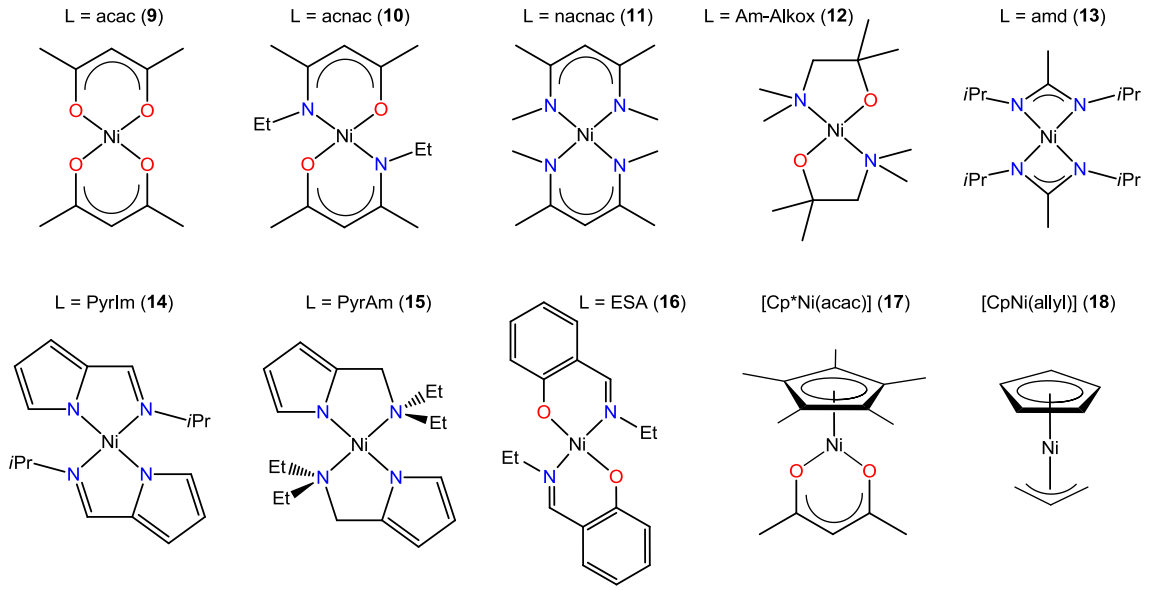

Figure 2. Nickel(II) complexes **9**-**18**.

Co-Reagents

Co-reagents investigated fall into two categories: (1) Si_2Me_6, Sn_2Me_6 and $B_2(Pin)_2$ (Pin = pinacolate = $OCMe_2CMe_2O$), and (2) $AlMe_3$, BEt_3 and $ZnEt_2$. The 1st category of co-reagent can be expected to yield unstable silyl, stannyl or boryl complexes via σ-bond metathesis, while reagents in the 2nd category can be anticipated to yield unstable alkyl derivatives by ligand exchange.

Solution Screening Reactions with Copper

Solution screening studies were performed by maintaining toluene solutions of precursors **1**-**8** with the six co-reagents described above. Reactions were performed using either 1 or 5 equivalents of co-reagent and were maintaned for 24 hours at each of the following temperatures in sequence: 25, 50, 75, 100 and 120 °C. Deposition of either a copper-colored metal film or precipitation of a black or copper-colored powder was observed at 25-50 °C in 88 % of the reactions with 5 equiv of $AlMe_3$ and $ZnEt_2$ (Figure 3). By contrast, BEt_3 and B_2Pin_2 reacted more slowly than the organoaluminium and organozinc reagents, Sn_2Me_6 required temperatures of 75 °C or higher, and Si_2Me_6 showed low reactivity.

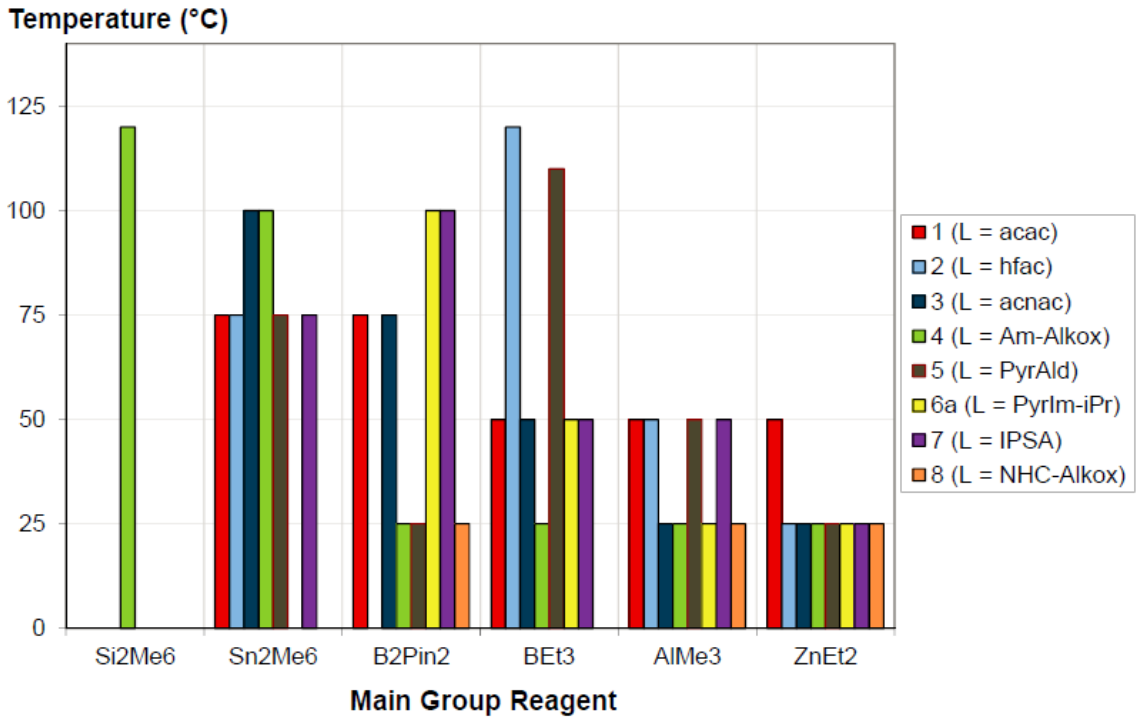

Figure 3. Minimum temperatures for deposition of a copper-containing film and/or powder.(22) Solutions were 10 mM (1.5 mL total volume) in copper complex, and reactions were maintained for 24 hours at each of the following temperatures in sequence: 25, 50, 75, 100, 120 °C. Bars at the baseline on the graphs correspond to complexes which did not deposit metal within the temperature range studied.

As described above, some metal precursor / ER_n co-reagent combinations yielded metal films while others produced powders. Selected reactions in the former category that employed the most reactive co-reagents, BEt_3, $AlMe_3$ and $ZnEt_2$, were repeated in the presence of $Si/SiO_2/Ta/Ru$ wafer sections, and the resulting films were analyzed by XPS after initial sputtering to remove higher levels of oxidized material and organic impurities at the surface. SEM images for a selection of the films are provided in Figure 4, along with visual appearance and elemental composition by XPS. These data are of independent interest from the perspective of solution deposition of metal films, and an understanding of film morphology is also valuable for the interpretation of XPS data. However, the morphology of solution-deposited films is not expected to correlate with film morphologies observed by ALD or pulsed-CVD.

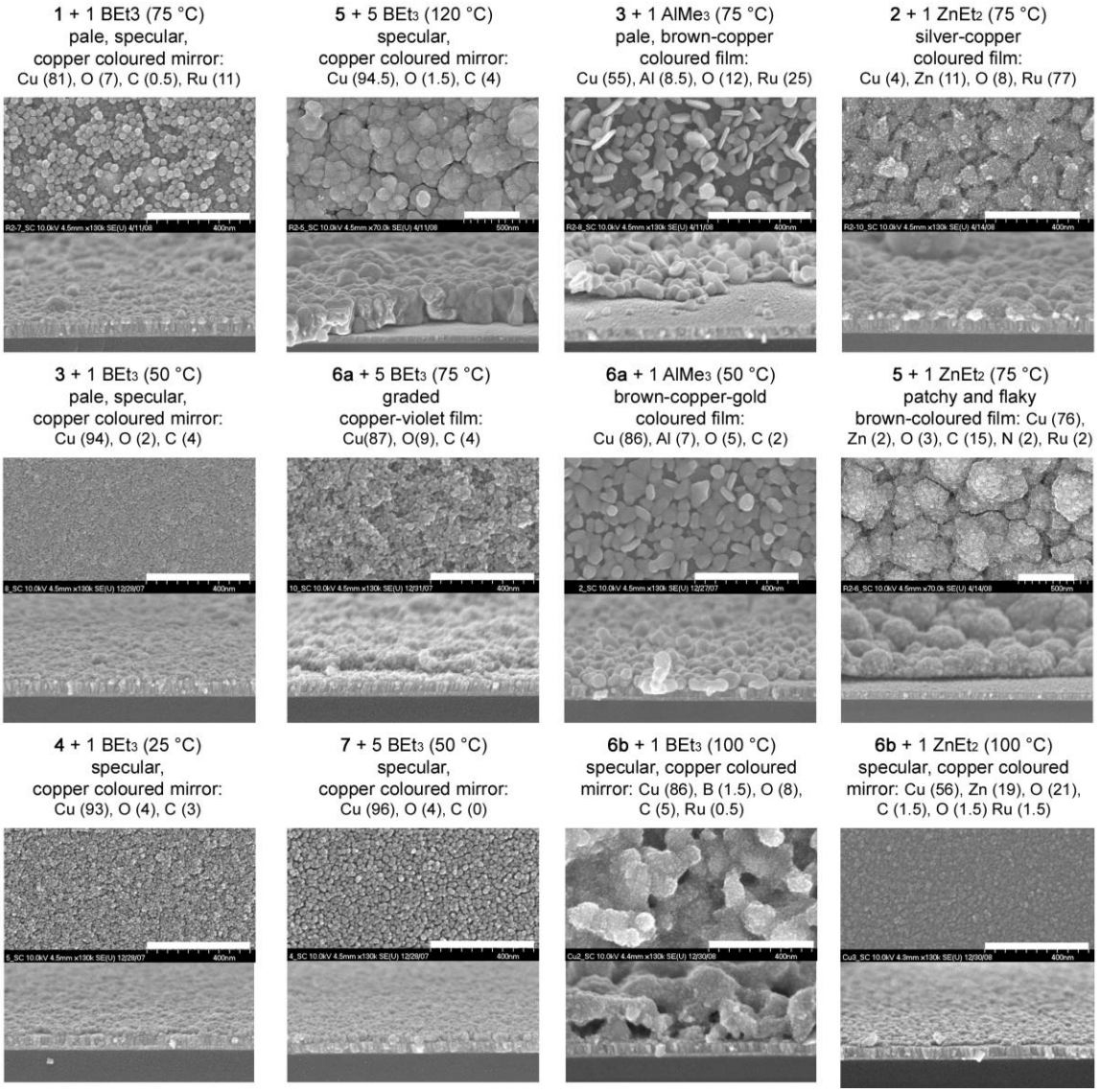

Figure 4. SEM images of selected metal films deposited on ruthenium through the reactions of **1-8** with ER_n co-reagents in toluene. For each film, the reagents, reaction stoichiometry, reaction temperature, macroscopic film appearance, and film composition (at% by XPS after sputtering until at% C and O values leveled off or the underlying Ru layer became apparent) are provided. White scale bars are set to 400 nm.

Key findings were: (1) All but one film (from the reaction of **5** with $ZnEt_2$) showed good adhesion to the substrate, as determined by a standard tape test. (2) Films were 10-300 nm thick with morphologies ranging from: dense solid films with an undulating surface, to continuous films of densely-packed approximately spherical 5-35 nm grains, to a loosely-packed layer of 30-130 nm diameter platelet-shaped granules (Figure 4). (3) Copper films deposited using BEt_3 contained very low levels of boron (0-1.5 at%) and did not contain nitrogen at levels detectable by XPS (~ 0.5 at%). (4) Metal films deposited using $AlMe_3$ contained < 0.5 at% N, but significant amounts of Al; from 8% to 42% Al in Cu. (5) Films deposited using $ZnEt_2$ contained varying amounts of Zn, with compositions ranging from 2.5% Zn in Cu, to predominantly Zn. (6) As is typically observed after

exposure to the atmosphere, oxygen was present in all films (typically 2–10 at% relative to Cu), including those prepared from oxygen-free precursors **6a** and **6b**. (7) Carbon was present in many of the films (e.g. 0–5% in films deposited using BEt_3 or $AlMe_3$). (8) The amount of oxygen and carbon in the films varied greatly depending on the amount of B, Al or Zn incorporated in the film, the susceptibility of each element to oxidation (Al > Zn > B), film thickness, and film morphology.

Metal powders deposited in the reactions of **1**-**8** with $AlMe_3$, BEt_3 and $ZnEt_2$ were also investigated, and were in most cases shown to be composed of copper by a combination of PXRD (which does not detect amorphous materials) and XPS.(23) These screening studies demonstrated the potential utility of $AlMe_3$, $ZnEt_2$, BEt_3 and B_2Pin_2 as new co-reagents for low temperature copper metal ALD or pulsed-CVD. They also highlighted the sensitivity of Cu film composition to the nature of the ligands in the $[CuL_2]$ precursor and the choice of ER_n co-reagent. However, it is important to note that in solution, films with lower B, Al or Zn content require the formation of *soluble* and thermally robust B-, Al- and Zn-byproducts, while in metal ALD or pulsed-CVD, byproduct *volatility* and thermal stability are key factors in determining the level of B, Al and Zn incorporation.

For some applications, incorporation of B, Al or Zn will be detrimental, while for others, it may be advantageous. For example, the benefits of alloying elements for copper interconnect applications have been discussed and aluminum is listed as one of ten elements (Pd, Au, Al, In, Ag, Cr, B, Ti, Nb and Mn) of particular interest in this role. Furthermore, zinc is included as one of six additional elements worthy of further investigation in this application (Zn, V, C, Mg, P and Sn).(24)

Solution Screening Reactions with Nickel

Solution screening studies were performed as described above for copper, and temperatures at which metal deposition was first observed are listed in Figure 5. A general trend is that nickel metal deposition generally required signficantly higher temperatures than were required for copper metal deposition using the same set of co-reagents. However, as was observed for copper, $ZnEt_2$ and $AlMe_3$ were the most reactive reagents while Si_2Me_6 was the least reactive. Selected precursor/co-reagent combinations which yielded a silver-coloured mirror were investigated by deposition from solution onto a Ni-seeded silicon wafer or H-terminated silicon wafer. These combinations were **16** with BEt_3, **16** with $ZnEt_2$, **12** with $ZnEt_2$ and **13** with $ZnEt_2$ at 100 °C. The reaction with BEt_3 yielded a smooth undulating film with a composition of 95 % nickel with the remainder being oxygen and carbon. By contrast, films deposited using $ZnEt_2$ were discontinuous, comprised of grains with a broad size distribution, and composed of an approximate 2:1 mixture of Ni:Zn(25) with 16-19 wt% oxygen (Figure 6).

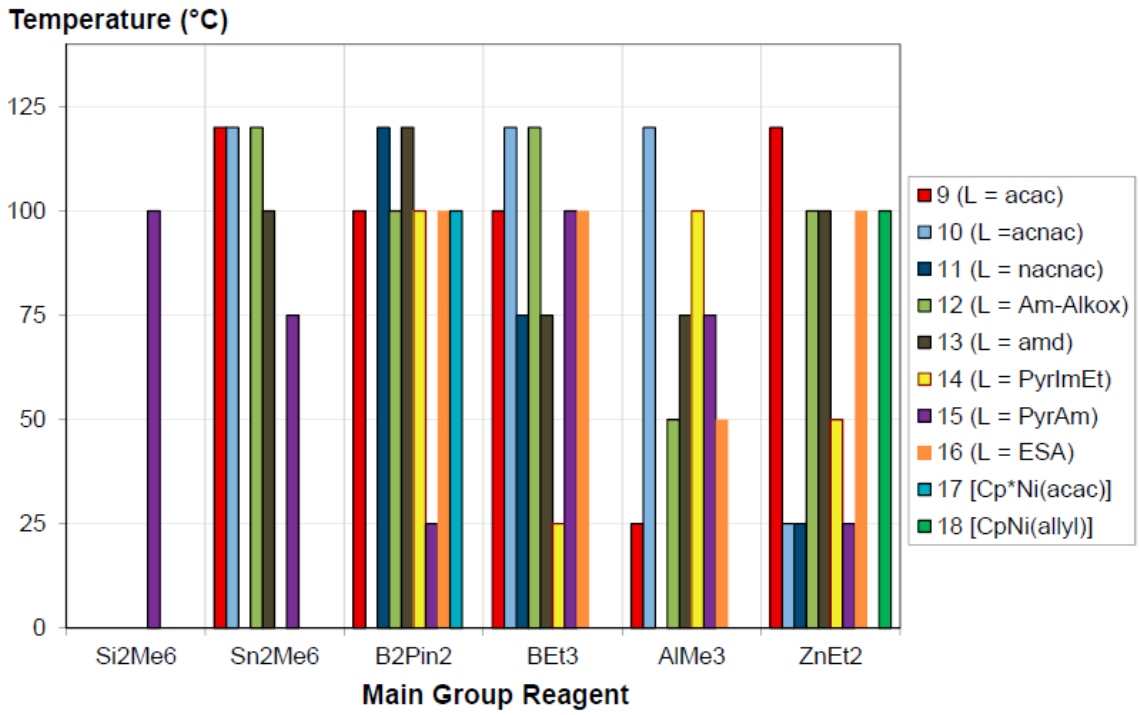

Figure 5. Minimum temperatures for deposition of a nickel-containing film and/or powder.(22) Solutions were 10 mM (1.5 mL total volume) in nickel complex, and reactions were maintained for 24 hours at each of the following temperatures in sequence: 25, 50, 75, 100, 120 °C. Bars at the baseline on the graphs correspond to complexes which did not deposit metal within the temperature range studied.

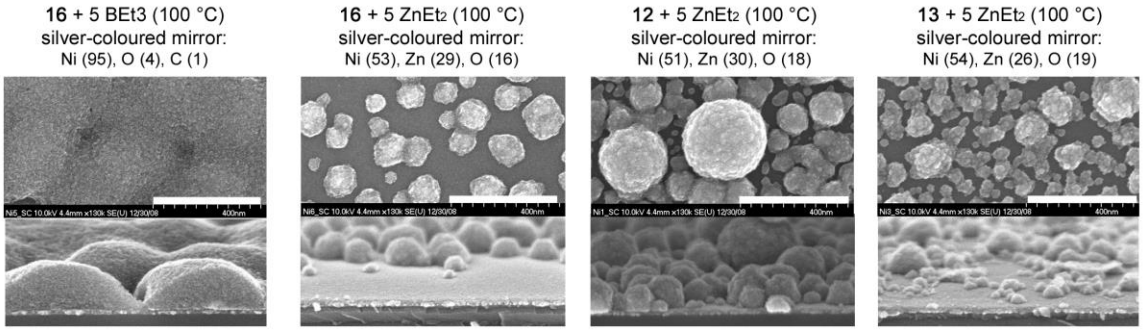

Figure 6. SEM images of selected metal films deposited on nickel-seeded silicon wafers through the reactions of **9-18** with ER_n co-reagents in toluene. For each film, the reagents, reaction stoichiometry, reaction temperature, macroscopic film appearance, and film composition (at% by XPS)(25) is provided. White scale bars are set to 400 nm.

ALD/pulsed-CVD Studies

Based on solution screening results as well as CuL_2 complex properties, precursors **6b** and **7** were selected for ALD/pulsed-CVD evaluation with the co-reagents $AlMe_3$, BEt_3 and $ZnEt_2$. Desirable features of these precursors are their volatility, the absence of fluorine in

the ligands, the absence of oxygen in the case of **6b**, and good thermal stability: CVD was not observed at 150 °C for **6b** and at 200 °C for **7**.

Deposition Studies using $AlMe_3$ as the Co-Reagent: At temperatures of 120 – 150 °C using **6b** with $AlMe_3$ as the co-reagent, copper-containing films were deposited via a pulsed-CVD mechanism. However, the resulting films were non-conductive and granular with a high Al and O content (after atmospheric exposure). The lack of electrical conductivity presumably stems from the presence of insulating Al_2O_3 (Al 2*s* binding energy of 119.0 eV). Since the ALD chamber received a two hour forming gas prebake at 250 °C prior to ALD/pulsed-CVD processing, the most likely source of Al_2O_3 in the film is the oxidation of metallic Al upon film exposure to air. Similar results were obtained using complex **7** in combination with $AlMe_3$ on both Ru and Ta substrates (150-180 °C), although in this case pilar-style growth was observed at 150 °C (Figure 7).

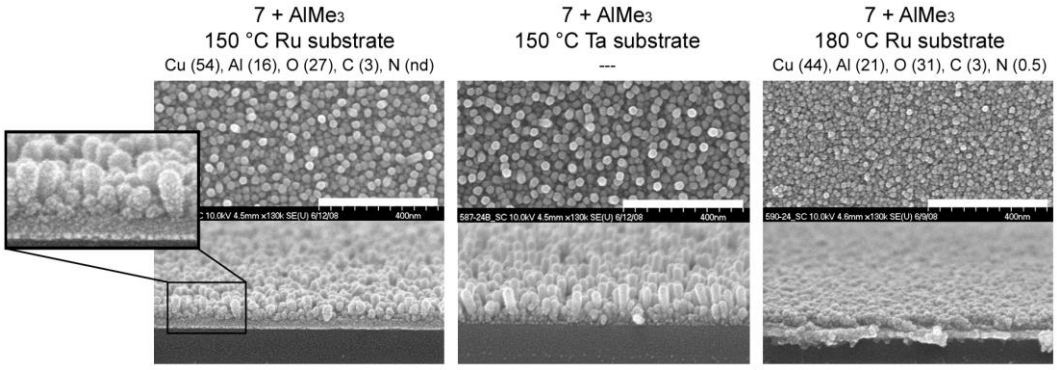

Figure 7. SEM images of films deposited at 150 and 180 °C on $Si/SiO_2/Ta/Ru$ or $Si/SiO_2/Ta$, using 5000 cycles of $AlMe_3$ / purge / complex **7** / purge. White scale bars are set to 400 nm. For films deposited on ruthenium, film compositions (at% determined by XPS after sputtering for 60 seconds) are shown in the caption (nd = not detected).

Deposition Studies using BEt_3 as the Co-Reagent: No deposition was observed when BEt_3 was used as a co-reagent with **6b** or **7** up to 150 °C. The observation of deposition with $AlMe_3$, but not BEt_3, is in keeping with the order of reactivity observed in solution ($AlMe_3$ >> BEt_3). However, factors such as ineffective chemisorption of BEt_3 vapors on the surface, or intial surface reactivity that does not result in the formation of active sites suitable to allow further film growth could also play an important role.

Deposition using $ZnEt_2$ as Co-Reagent: With $ZnEt_2$ in combination with **6b**, conductive copper films were deposited from 120 °C to 150 °C on SiO_2, PVD Ta and PVD Ru substrates. All films are granular with low carbon impurities post sputter (< 2 at%) and no detectable nitrogen, suggesting minimal incorporation of the *N*-ethyl-2-pyrrolylaldiminate or ethyl ligands. In a typical deposition, a pulse sequence consisting of a 6s pulse of $ZnEt_2$ followed by a 7s chamber purge, a 3s pulse of **6b** and a final 7s chamber purge yielded granular films with a growth per cycle of approximately 0.1 Å. As is evident in the SEM images presented in Figure 8, films deposited on SiO_2 and PVD Ta substrates at 130 °C are both smooth and uniform. Four point probe sheet resistance measurement of the film on SiO_2 combined with a thickness of 120 Å yielded a resistivity of 89 μΩ·cm.

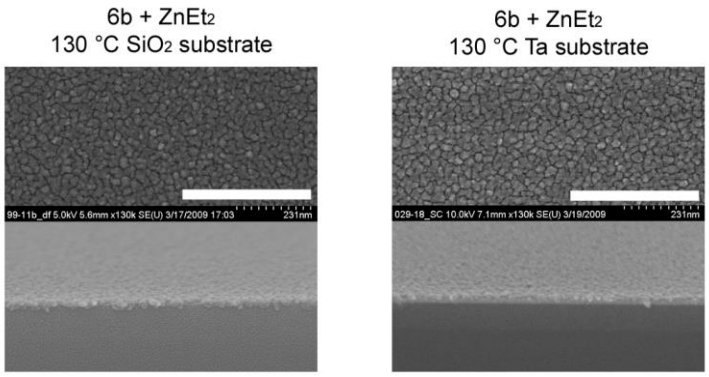

Figure 8. SEM images of films deposited at 130 °C on SiO_2 and PVD Ta, respectively, using 1500 cycles of: 6s pulse $ZnEt_2$ / 7s chamber purge / 3s pulse of **6b** / 7s chamber purge. White scale bars are set to 400 nm.

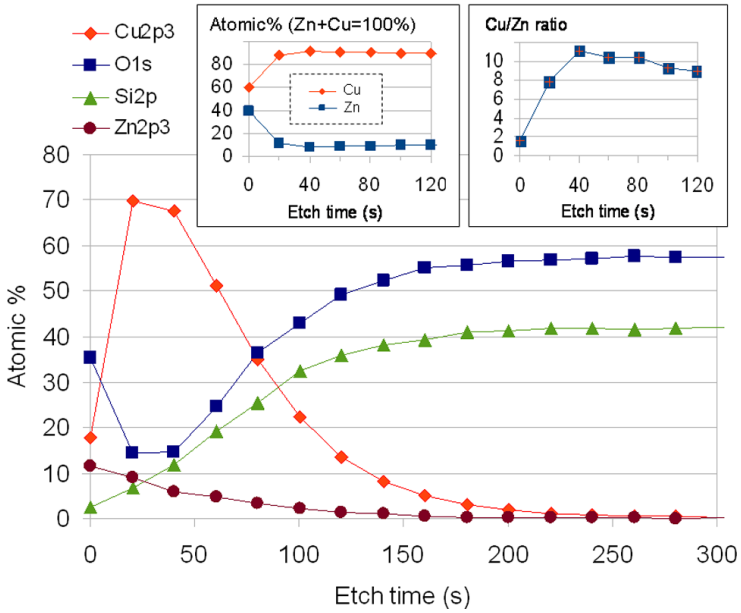

Figure 9. XPS determined atomic% compositional depth profile [carbon values were < 2 at% at all sputter depths (20 – 300 s), so are not included in the profile] of film deposited on SiO_2 at 130 °C using 1500 cycles of the following pulse sequence: 6s pulse $ZnEt_2$ / 7s chamber purge / 3s pulse of **6b** / 7s chamber purge. The inset on the left plots Zn atomic% and Cu atomic% where the total Zn and Cu content is set to 100%. The inset on the right plots the Cu:Zn ratio against etch time.

The composition of the film deposited on SiO_2 at 130 °C was analyzed by XPS depth profiling which revealed that Zn was the main film impurity, with no detectable N and less than 2 at% C detected at all sputter depths. Some interesting trends were apparent in the elemental depth profiling (Figure 9). Most prominently, the outer surface of the film was richer in Zn compared to the bulk of the film where a significantly higher concentration of copper was detected. Oxygen was detected at all levels of the depth profile, but the Si/O ratio remains constant after sputtering for 40s, which suggests that in the bulk of the film, copper and zinc are predominantly in metallic form. The observed electrical conductivity of

the film also supports the presence of a substantial amount of metallic Cu and/or Zn in the film, most likely alloyed as a brass. As the depth profile shows, the ratio of Cu/Zn in the film was maximized at approximately 11:1. Attempts to further increase the concentration of Cu in the film by varying the substrate temperature between 130 °C and 150 °C, or the length of purges or precursor/co-reactant doses led only to Cu:Zn ratios between 6 and 12.

The observed Zn content in the film suggests that reductive decomposition of $ZnEt_2$ (or its transmetallation products) is occurring as has been suggested for the $ZnEt_2/H_2O$ ALD ZnO process.(26) Moreover, the increase in Zn concentration close to the surface of the film suggests that this process is self-catalyzed. However, it is also possible that Zn 'percolates' to the surface of the film as it grows, leading to a higher Zn concentration near the surface, even if the Cu/Zn ratio for material added in each deposition cycle remains constant. This type of 'surfactant' behaviour has previously been reported for C in Zn,(27) I in Cu,(28) and Bi_2O_3 in $LaAlO_3$.(29)

To gain insight into the process of zinc incorporation into the films, CVD of Zn on a copper substrate was attempted at 100-170 °C (Figure 10). At 100 and 120 °C, only a small amount of Zn deposition was observed after 1000 × 1 s pulses, while at 140 and 170 °C, CVD of large grains on the surface was observed (zinc deposition was confirmed by XPS). It therefore appears that in ALD/pulsed-CVD experiments using **6b** in combination with $ZnEt_2$, zinc incorporation occurs via a parasitic CVD pathway(30) that becomes far more pronounced at temperatures of 120 °C and above, detracting from the goal of self-limiting deposition (i.e. leading to a pulsed CVD rather than an ALD process). Consistent with this interpretation, Sung, Koo and Fischer *et al.* reported pure copper metal ALD using $[Cu(OCHMeCH_2NMe_2)_2]$ in combination with $ZnEt_2$ at 100 to 120 °C, while substantial zinc incorporation was observed above 120 °C.(31) Unfortunately, with complex **6b**, similarly low deposition temperatures were not accessible due to a minimum precursor delivery temperature of 120 °C.

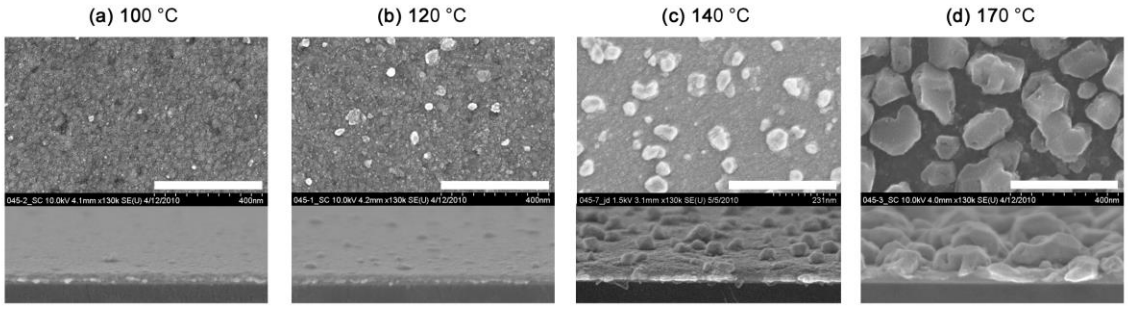

Figure 10. SEM images of CVD films deposited on PVD-Cu using $ZnEt_2$ at 100 - 170 °C. Depositions were run using 1000 cycles × [1s pulse $ZnEt_2$ / 3s chamber purge].

Solution NMR Studies

To provide a starting point for the analysis and understanding of surface reactivity responsible for metal ALD/pulsed-CVD, the solution reactions of $[Cu(PyrIm^{iPr})_2]$ (**6a**) with $AlMe_3$, BEt_3 and $ZnEt_2$ were studied using ^1H NMR spectroscopy over a range of temperatures with various copper precursor / ER_n co-reagent ratios.(8) The formation or absence of hydrogen, methane, ethane, ethylene and/or *n*-butane was determined by comparison of ^1H and/or ^{13}C NMR chemical shifts with literature values (using gas-tight J. Young NMR tubes) and ^1H NMR after purging with argon gas. All other stable organic and inorganic intermediates and by-products were assigned by comparison with

independently synthesized and characterized samples. In each case, reduction occurs in two stages via a stable dinuclear copper(I) pyrrolylaldiminate complex, $[Cu_2(PyrIm^{iPr})_2]$ (**19**; Figure 11), with each stage initiated by copper alkyl complex formation. Reaction pathways responsible for copper metal deposition in reactions of **6a** with $ZnEt_2$ are shown in Figure 11.

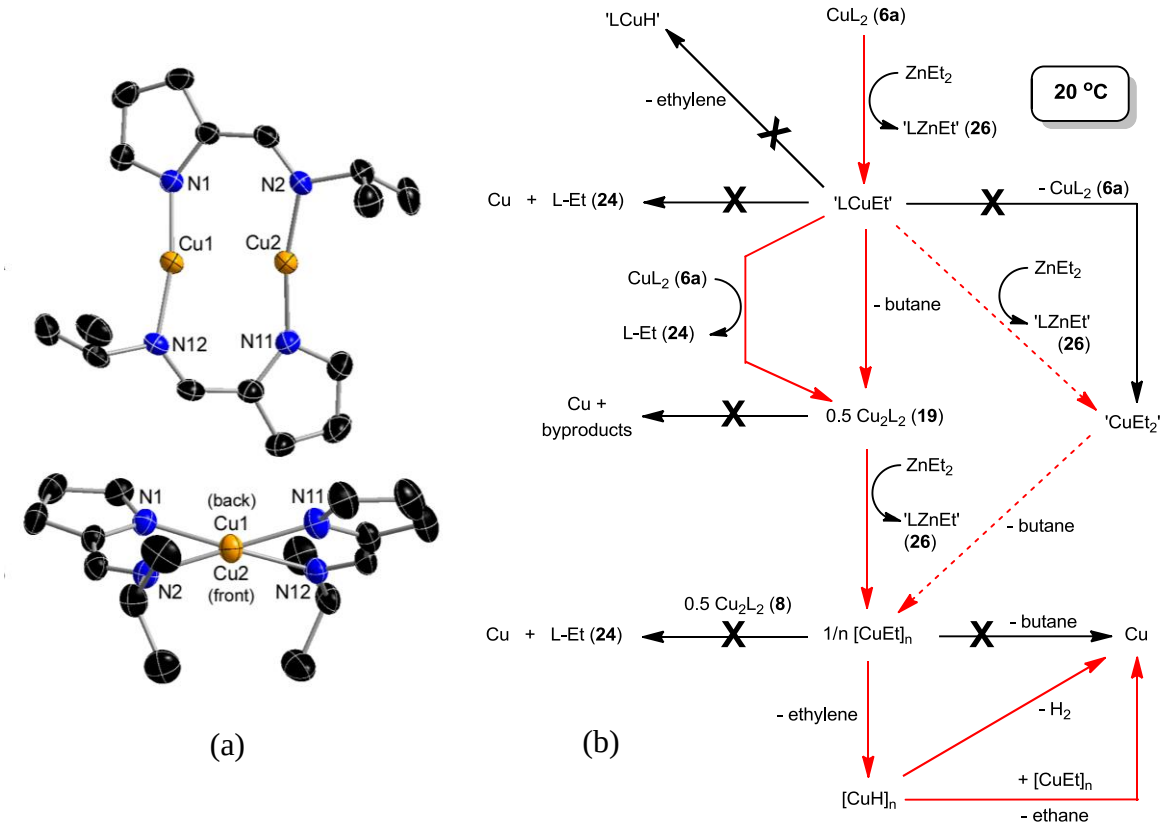

Figure 11. (a) 2 views of the X-ray crystal structure of $[Cu_2(PyrIm^{iPr})_2]$ (**19**). (b) Reaction Pathways for Copper Metal Deposition from **6a** with $ZnEt_2$ (L = $PyrIm^{iPr}$). Reactions marked with an 'X' do not occur. Dotted arrows represent reactions that cannot be ruled out in the presence of a large excess of $ZnEt_2$.

In reactions with $ZnEt_2$, BEt_3 and $AlMe_3$, the first step is presumably conversion of **6a** to '$(PyrIm^{iPr})CuR$' by ligand exchange between the copper precursor and organometallic co-reagent. This undetected intermediate then decomposes rapidly to yield $[Cu_2(PyrIm^{iPr})_2]$ (**19**) with release of R_2 or $PyrIm^{iPr}$-R, consistent with bimolecular C–C or C–N bond forming reductive elimination. Complex **19** was then converted to thermally unstable 'CuR' by ligand exchange between **19** and the organometallic co-reagent. At room temperature or below, copper deposition from 'CuMe' occurs exclusively via reductive elimination of ethane, while decomposition of 'CuEt' yields ethylene, ethane and hydrogen, indicative of β-hydride elimination followed by reductive elimination. In the presence of an excess of the more reactive reagents $AlMe_3$ and $ZnEt_2$, it was not possible to rule out initial double alkylation to form a highly unstable copper(II) dialkyl species. However, if 'CuR_2' does form, it must decompose to 'CuR' rather than to copper metal, since under these conditions (an excess of $AlMe_3$ or $ZnEt_2$),

copper metal formation is not observed at temperatures where 'CuR' is stable. The intermediates and byproducts [$Cu_2(PyrIm^{iPr})_2$] (**19**), [$(PyrIm^{iPr})AlMe_2$] (**20**), [$(PyrIm^{iPr})_2AlMe$] (**21**), [$Al(PyrIm^{iPr})_3$] (**22**), $PyrIm^{iPr}$-Me (**23**), $PyrIm^{iPr}$-Et (**24**), [$(PyrIm^{iPr})BEt_2$] (**25**), [$(PyrIm^{iPr})ZnEt$] (**26**) and [$Zn(PyrIm^{iPr})_2$] (**27**) were prepared independently in pure form, and characterized by NMR spectroscopy and in some cases X-ray crystallography.(8) All byproducts are thermally stable, with the exception of **26** which undergoes ligand redistribution to form **27** and $ZnEt_2$ at elevated temperatures and in solution. Of the stable organometallic complexes, mono-ligated **20** and **25** are the most volatile, so are particularly desirable as byproducts in ALD or pulsed-CVD.

Summary and Conclusions

Solution deposition studies identified $ZnEt_2$ and $AlMe_3$ as particularly promising co-reagents for copper metal ALD/pulsed-CVD when combined with copper(II) precursors. Subsequent ALD/pulsed-CVD using $ZnEt_2$ with bis(*N*-ethyl-2-pyrrolylaldiminate)copper(II) (**6b**) yielded conductive copper metal films at 130–150 °C. For films deposited on SiO_2 at 130 °C using a typical pulse sequence, XPS depth profiling revealed that Zn was the main film impurity, with no detectable N and less than 2 at% C detected at all sputter depths. The maximum copper/zinc ratio was approximately 11:1, with a significant decrease in this ratio near the surface of the film.

CVD studies with $ZnEt_2$ point towards the operation of parastic $ZnEt_2$ reduction pathways that become particularly significant at temperatures above 120 °C. Nevertheless, this work highlights the potential of $ZnEt_2$ and related volatile organometallics as co-reagents for low-temperature late transition metal ALD and pulsed-CVD, and demonstrates the successful implementation of solution screening tests to define the focus of ALD/pulsed-CVD studies. It is also worth noting that BEt_3 demonstrated significantly lower reactivity as a co-reagent than $ZnEt_2$ or $AlMe_3$ in solution, and this translated into a lack of reactivity between BEt_3 and **6b** or **7** in attempted ALD/pulsed-CVD reactions at temperatures up to 150 °C.

Detailed NMR spectroscopic studies were carried out to elucidate the pathways responsible for the deposition of copper metal from solution using **6a** in combination with $ZnEt_2$, $AlMe_3$ and BEt_3. All stable intermediates and byproducts were independently prepared to allow conclusive identification. Key copper-containing intermediates were 'LCuR', [Cu_2L_2] and [$CuR]_n$, with each 1-electron reduction step taking place by C–C, C–N, C–H or H–H bond-forming bimolecular reductive elimination.

Acknowledgments

DJHE is grateful for funding provided by Intel Corporation and the Emerging Materials Knowledge (EMK) program of Ontario Centres of Excellence (OCE), Canada.

References

1. A. C. Jones and M. L. Hitchman, in *Chemical Vapour Deposition: Precursors, Processes and Applications*, RSC Publishing, Cambridge, (2009).
2. M. Ritala and M. Leskelä, in *Atomic Layer Deposition*: *Handbook of Thin Film Materials*, Vol. 1 - Deposition and Processing of Thin Films, H. S. Nalwa, Editor, Academic Press: San Diego (2001).
3. B. Vidjayacoumar, D. J. H. Emslie, S. B. Clendenning, J. M. Blackwell, J. F. Britten and A. Rheingold, *Chem. Mater.*, **22**, 4844 (2010).
4. J. Cheon, D. M. Rogers and G. S. Girolami, *J. Am. Chem. Soc.*, **119**, 6804 (1997).
5. W. R. Entley, C. R. Treadway, S. R. Wilson and G. S. Girolami, *J. Am. Chem. Soc.*, **119**, 6251 (1997).
6. C. D. Tagge, R. D. Simpson, R. G. Bergman, M. J. Hostetler, G. S. Girolami and R. G. Nuzzo, *J. Am. Chem. Soc.*, **118**, 2634 (1996).
7. Y. P. Zhang, Z. Yuan and R. J. Puddephatt, *Chem. Mater.*, **10**, 2293 (1998).
8. B. Vidjayacoumar, D. J. H. Emslie, J. M. Blackwell, S. B. Clendenning and J. F. Britten, *Chem. Mater.*, **22**, 4854 (2010).
9. G. J. Bullen, R. Mason and P. Pauling, *Inorg. Chem.*, **4**, 456 (1965).
10. G. W. Everett, Jr. and R. H. Holm, *J. Am. Chem. Soc.*, **87**, 2117 (1965).
11. S. G. McGeachin, *Can. J. Chem.*, **46**, 1903 (1968).
12. B. S. Lim, A. Rahtu, J.-S. Park and R. G. Gordon, *Inorg. Chem.*, **42**, 7951 (2003).
13. S. H. Yoo, H. Choi, H. S. Kim, B. K. Park, S. S. Lee, K. S. An, Y. K. Lee, T. M. Chung and C. G. Kim, *Eur. J. Inorg. Chem.*, 1833 (2011).
14. P. Werndrup, S. Gohil, V. G. Kessler, M. Kritikos and L. G. Hubert-Pfalzgraf, *Polyhedron*, **20**, 2163 (2001).
15. R. H. Holm, A. Chakravorty and L. J. Theriot, *Inorg. Chem.*, **5**, 625 (1966).
16. H. Drevs, A. Schmeisser, H. Hartung and U. Baumeister, *Chem. Ber.*, **129**, 853 (1996).
17. L. Sacconi, P. Paoletti and D. R. Guiseppe, *J. Am. Chem. Soc.*, **79**, 4062 (1957).
18. T. Akitsu and Y. Einaga, *Polyhedron*, **24**, 1869 (2005).
19. E. E. Bunel, L. Valle and J. M. Manriquez, *Organometallics*, **4**, 1680 (1985).
20. W. R. McClellan, H. H. Hoenh, H. N. Cripps, E. L. Muetterties and B. W. Howk, *J. Am. Chem. Soc.*, **83**, 1601 (1961).
21. A. Kermagoret and P. Braunstein, *Organometallics*, **27**, 88 (2008).
22. Successful metal deposition is only reported in Figures 3 and 5 when a significant quantity of copper was deposited by visual inspection. Given that each reaction involved only 4-6 mg (15 μmol) of the copper precursor, this corresponds to deposition of a substantial percentage of the copper metal present.
23. Colloidal brass (5-65 at% Zn in Cu) has been prepared either by addition of an octylamine solution of $[Cu(OCHMeCH_2NMe_2)_2]$ and $ZnEt_2$ to hexadecylamine at 250 °C, or by sequential addition of octylamine solutions of $[Cu(OCHMeCH_2NMe_2)_2]$ and then $ZnEt_2$ to hexadecylamine at 250 °C. Pure colloidal copper and zinc were also accessible by addition of an octylamine solution of just $[Cu(OCHMeCH_2NMe_2)_2]$ or $ZnEt_2$ to hexadecylamine at 250 °C: J. Hambrock, M. K. Schröter, A. Birkner, C. Wöll, R. A. Fischer, *Chem. Mat.*, **15**, 4217 (2003).
24. K. Barmak, C. Cabral, Jr., K. P. Rodbell and J. M. E. Harper, *J. Vac. Sci. Technol., B*, **24**, 2485 (2006).

25. For films deposited on nickel-seeded silicon wafers using $ZnEt_2$ as the co-reagent, the at% of Ni measured by XPS will be higher than that in the deposited material due to the discontinuous nature of the films.
26. P. C. Rowlette, C. G. Allen, O. B. Bromley, A. E. Dubetz, C. A. Wolden, *Chem. Vap. Deposition*, **15**, 15 (2009) and references therein.
27. J. Cheon, L. H. Dubois and G. S. Girolami, *Chem. Mater.*, **6**, 2279 (1994).
28. T.-Y. Chang, J.-J. Tze and D.-S. Tsai, *Appl. Surf. Sci.*, **236**, 165 (2004).
29. A. A. Molodyk, I. E. Korsakov, M. A. Novojilov, I. E. Graboy, A. R. Kaul and G. Wahl, *Chem. Vap. Deposition*, **6**, 133 (2000).
30. M. Juppo, M. Ritala and M. Leskelä, *J. Vac. Sci. Technol. A*, **15**, 2330 (1997).
31. B. H. Lee, J. K. Hwang, J. W. Nam, S. U. Lee, J. T. Kim, S.-M. Koo, A. Baunemann, R. A. Fischer and M. M. Sung, *Angew. Chem. Int. Ed.*, **48**, 4536 (2009).